SSC-SR-1031

The Superconducting Super Collider

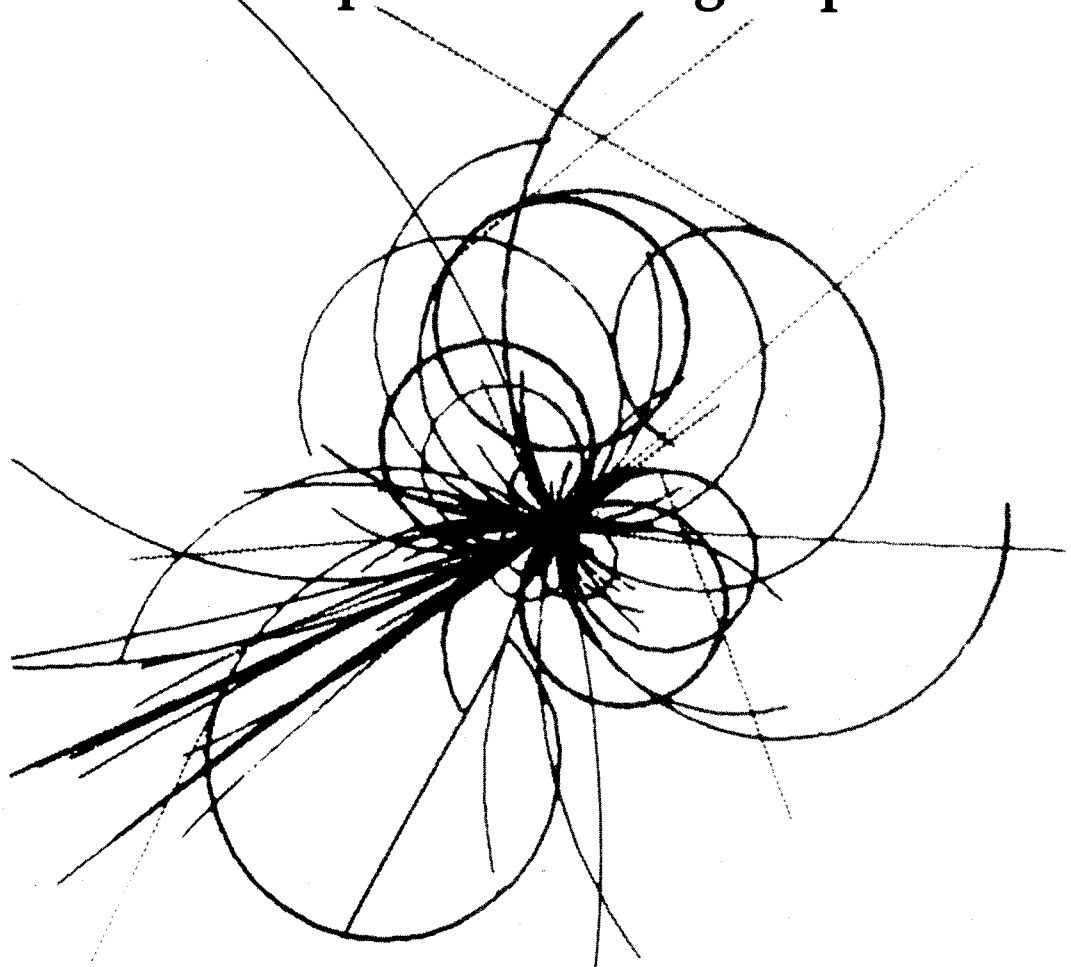

Workshop on Radiological Aspects of SSC Operations

Task Force Report

T.E. Toohig, Editor
SSC Central Design Group

May 1987

SSC-SR-1031

WORKSHOP ON RADIOLOGICAL ASPECTS OF SSC OPERATIONS

Task Force Report

T. E. Toohig, Editor

SSC Central Design Group*
c/o Lawrence Berkeley Laboratory, 1 Cyclotron Road, Berkeley, CA 94720

May 1987

*Operated by Universities Research Association for the U.S. Department of Energy

PREFACE

A workshop in Radiological Aspects of SSC Operations was hosted by the SSC Central Design Group at the Lawrence Berkeley Laboratory May 4-6, 1987. This workshop was intended to complement the SSC workshop on Environmental Radiation which took place at the CDG from October 14-16, 1985.

The present report represents a summary of the large amount of material that was presented at the workshop. The great bulk of the material is contained in the voluminous appendices.

To make this material accessible, sets of these appendices will be maintained at the CDG, at Fermilab, and at CERN. Copies of selected appendices may be requested from CDG.

RADIOLOGICAL ASPECTS OF SSC OPERATIONS

PARTICIPANTS

Sam Baker, Fermilab
Robert Casey, BNL
Donald Cossairt, Fermilab
Per Dahl, CDG/BNL
Alberto Fasso, CERN
William S. Freeman, Fermilab
Don Groom, SSC/CDG
Ted Jenkins, SLAC
Joe McCaslin, LBL
Lutz, Moritz, TRIUMF
R. Nelsen, ANL
Keran O'Brien, Retired
Jim Opelka, ANL
Jack Riddle, RTK
Jim Sanford, SSC/CDG
Gary Schleimer, LBL
Geoffrey Stapleton, CEBAF
Alan Stevens, BNL
Graham R. Stevenson, CERN
William P. Swanson, LBL
Tim Toohig, SSC/CDG
Ralph Thomas, LBL
Paula Trinoskey, RTK
Andreas Van Ginneken, Fermilab
Harold Wollenberg, LBL

		Page
Preface		i
List of Participants		ii
Table of Contents		iii
Chapter 1.	Introduction	1
Chapter 2.	Environment and Monitoring	3
2.1	Neutron Skyshine	3
2.2	Off-site Muons	9
2.3	Gas, Dust and Aerosol Activation	11
2.4	Ground Water Activation	13
2.5	Philosophy of Environmental Monitoring	16
2.6	Conclusions and Recommendations	17
Chapter 3.	Superconducting Components	19
3.1	Energy Deposition Calculations for the LHC Dipole	19
3.2	Monte Carlo Calculations of Radiation-Induced Heating in Magnets	21
3.3	Measurement of Neutron Spectra in the Tevatron Tunnel	23
3.4	Implications for the SSC	25
3.5	Issues/Future Studies	26
3.6	Conclusions	28
Chapter 4.	Primary Beam Absorbers	30
4.1	Summary of Presentations	30
4.2	Implications for the SSC	32
4.3	Suggestions for Future Studies	34
4.4	Conclusions	35

Chapter 5. Interaction Regions 37
5.1 Radiation Dose to Detectors 37
5.2 Labyrinths, Ducts, and Penetrations 39
5.3 Lateral Hadron Shielding 41
5.4 Problems with Depleted Uranium 44
5.5 Accidental Uranium Release 45
5.6 Accelerator Shielding Prospectives 46
5.7 Issues, Future Study and Conclusions 48

References 53
List of Appendices 55

Chapter 1

INTRODUCTION

Integral to the design of an accelerator facility is the provision of adequate shielding to contain any radiation arising from operation of the facility. Study of the shielding requirements for the SSC have been an integral part of its design from its inception.[1] Concomitant with the evolution of the design of the accelerator, the design of the shielding was modified to reflect the accelerator design and the evolving understanding of the shielding requirements in this new energy range. This evolution is reflected in the Reference Designs Study[2] and in the conceptual Design Report.[3] Further definition of criteria leading up to the Invitation for Site Proposals[4] were examined in a workshop on SSC Environmental Radiation[5] and by a Task Force on Environmental Radiation Shielding.[6]

Complementary to the questions of environmental shielding are a number of radiation questions related to operation of the completed facility. One obvious need is the specification of systems for monitoring environmental emissions to ensure consistency between the design criteria and the actual levels during operation. Another question is the effect on the components of the machine of the radiation within the environmental shield. A workshop on Radiological Aspects of SSC Operations was convened to examine these questions at the SSC Central Design Group in Berkeley, May 4-6, 1987, drawing on the experience of the major North American and European accelerator laboratories.

Chapter 2

ENVIRONMENT AND MONITORING

2.1 Neutron Skyshine

Skyshine is the term used to describe neutron radiation emerging more or less vertically from a shielded enclosure which scatters from air molecules to produce radiation at some distance from the source.

Two empirical formulae are widely used to summarize the experimental data.[7-9] These formulae have different behavior at large distances

$$H(r) = \frac{a\, e^{-r/\lambda}}{r^2} \tag{1}$$

and

$$H(r) = \frac{b\, e^{-r/\lambda}}{r} . \tag{2}$$

λ has values between 140 and 120 m in the published literature. Qualitative explanations of these values for λ may be found in the source neutron spectrum.

Both representations derive from early theoretical work by Lindenbaum,[10] the first term [Eq. (1)] representing the direct (uncollided) neutron component and the second term representing the diffusion component. Moyer[7] showed that both components exhibit a similar variation with distance up to distances of 1 kilometer from the source. Experimental data are analyzed using either form Eq. (1) or (2) but do not have sufficient accuracy to successfully distinguish between them. Analysis is complicated by the fact that many published data consist of a mixture of direct and diffusely scattered neutrons. (See Appendix A.7)

Stapleton (CEBAF) has found that the formulations of Eqs. (1) and (2) can predict dose-equivalent rates which differ by an order of magnitude at distances of 150 m from the radiation source. Such apparent differences are disquieting rather than serious, but efforts are under way at CEBAF to understand them and, if possible, produce a single formulation of skyshine which will successfully describe the observed data.

Beam losses in enclosures with relatively thin roof shields will result in source neutrons passing through the roof to be scattered in the air above to give rise to radiation doses outside at ground level, and at considerable distances from the enclosure.

The basic production mechanisms of the roof neutrons comprise the original source evaporation (low energy) neutrons together with neutrons created in the roof material and in the air above the roof by the high energy component of the source neutrons. The complex nature of the phenomena together with the energy dependence of the scattering and absorption cross sections makes it difficult to derive a simple analytical model for the phenomenon. Analogy with low energy (fast and thermal), studies suggest that skyshine could best be described by diffusion theory. This results in a $1/r$ representation with distance. Other authorities have, however, utilized a $1/r^2$ formulation.

Jenkins (SLAC) confirmed that the normalized formulations of Eqs. (1) and (2) produce similar results at distance of ~350 meters from the radiation source. At the SSC, the penetrations through the shield would give rise to sources of relatively low energy neutrons. In such cases, diffusion theory might be expected to reasonably describe the radial variation of dose equivalent. (Ladu et al., showed the Monte-Carlo calculations for 5 MeV

neutrons gave results in essential agreement with Lindenbaum's diffusion equation.) Jenkins suggested that existing neutron transport codes, such as MORSE and Sandia's SKYSHINE, were entirely adequate to determine the neutron spectrum and fluence rate emerging from labyrinths and shield-penetrations.[5] Cross-section data bases extend up to 400 MeV. For SSC, the refrigerator stations did not appear to be a significant source of skyshine; the experimental area facility buildings, with their low beam loss, similarly did not seem to be a significant radiation source. However, given a reduction in source to boundary distance, this would become an issue to be revised.

Stevenson (CERN) mentioned the success of Alsmiller's DOT calculations and the tabulated data (Appendix D.8). Experience at the SPS has shown that the 9-m diameter shafts may be simply treated as point sources at the ground surface. Inverse square variation of dose equivalent with distance from the shaft provides a conservative estimate -- with no significant problems. Measurements of neutron spectra along the labyrinths are now available from Bonner-spectrometer data at FNAL (Appendix A.17). These data could be used to provide the neutron spectrum emerging from shield penetrations. Furthermore, properly designed penetrations have low-energy neutron leakage spectra (unlike the roof shielding transmission spectra, which extends to high energies). For the low energy leakage spectra, the transmission of neutrons through the atmosphere is well understood.

Stapleton (CEBAF) has found by using the various representations of skyshine differences in dose equivalent rates of an order of magnitude. These differences mainly relate to roof thickness where, for thin roofs the evaporation neutrons from the primary source dominate; and, for thick roofs,

where the creation of new neutrons in the roof material assume greater importance. Such apparent differences require resolution; efforts are underway at CEBAF to understand and reconcile these differences and to produce a formulation of skyshine that will fully describe the observed data.

Cossairt (FNAL) summarized skyshine measurements at Fermilab (Appendix A.14). Estimates of source strength (integrated over the shield roof) have been analyzed in terms of the empirical representation

$$H(r) = \frac{a\ Q\ (1-e^{-r/\mu})}{r^2}\ e^{-r/\lambda} \quad ,$$

with μ = 56 m and λ usually has a value of about 300 m but can take a value as high as 1200 m for poorly covered sources emitting a "hard" spectrum.

Cossairt also reported his estimates of skyshine from SSC Interaction Regions (Appendix A.16). With quite conservative beam loss assumptions, extreme values of skyshine dose equivalent at a distance of 1 kilometer range between 1 and 10 millirem per annum. However, Cossairt did not make any estimate of the attenuation of radiation provided by the massive detectors that will always be in place during SSC operation. This attenuation will reduce Cossairt's calculated dose equivalent rates by at least a factor of 100.

SUMMARY OF COMMENTS OF SKYSHINE

1. SLAC is a "true" skyshine geometry (no direct line-of-sight). We've measured skyshine out to 730 m distance. These measurements can be fit by the Lindenbaum formulation of the form

$$\frac{K}{r}\ e^{-r/\lambda} \quad \text{with } \lambda \sim 140 \text{ m},$$

which agrees with DESY measurements (DESY not necessarily being a true skyshine measurement). It can also be fit with the formulation

$$\frac{K}{r^2}\ e^{-r/\lambda}\ , \text{ using a } \lambda \text{ value of 150 m.}$$

Recent measurements at ISN, Japan by Nakamura et al., have also been fit using the $1/r$ instead of $1/r^2$ method. None of the above data work well using the $1/r^2$ formulation if λ is as large as 850 m, such as has been suggested for proton machines. So the method used, $1/r$ or $1/r^2$ doesn't seem to be as critical as the value of λ chosen, and indeed, with appropriate manipulation, one can fit most of the available data with one formula or another.

2. For geometries that aren't truly "skyshine" only, but include a direct component, one should expect a $1/r^2$ character. Furthermore, one should be able to calculate the source term at the surface and take it into 2π fairly simply. Note that in this case particularly, one must include the attenuation of neutrons (of a near MeV energy) in air; i.e., with a mean free path of ~50 m.

3. For all small penetrations, (i.e., exhaust ducts, cryogenic ports, stairwells, etc.), there will be no high-energy component, but only the lower energy neutrons (i.e., from evaporation) need to be considered. The ducting of these are well understood, and they form a source term that can be used easily for skyshine purposes.

4. There are various codes available that can be used to calculate skyshine assuming the source term is well known. Some are dedicated skyshine codes (SKYSHINE from Sandia, for example); others are excellent for this purpose, such as MORSE. They work mostly in the evaporation neutron-to-thermal neutron energy range, but this should be adequate for most of SSC's needs. For example, the Interaction Region areas will have large detectors which absorb most of the higher energy neutrons produced in beam-beam interactions. (There should be no other losses in the IR's, leaving only low energy neutrons to reach the roofs.)

2.2 Off-Site Muons

Freeman (FNAL) reported measurements of muon fluence rates downstream of experimental beams (Appendix A.8). A portable muon telescope (two 20 cm x 20 cm x 0.25 in. plastic scintillators) -- mounted in a van -- was used to determine muon beam profiles. Radiation levels at the Fermilab site boundary, at ground level, ranged from 0.04 to 3 millirem per year, during the period 1978 - 1985. Because of the orientation of the muon beams, dose equivalent rates may be as much as an order of magnitude higher at distances of up to 50 feet above local ground level.

Predictions of muon dose rates using CASIM and HALO are in fair agreement with the experimental observations (better than a factor 5 in most cases). There was general agreement that HALO was a difficult and laborious beam transport code in practice. Perhaps, effort could be given to the development of a more appropriate and 'user-friendly' code -- dedicated to the purpose of predicting environmental muon dose-equivalent rates from well-known radiation sources.

The environmental monitoring of muons appears to pose no serious technical problems. Total external loss LET (photon plus muon) radiation intensities may be measured using high-pressure ionization chambers or large volume, ambient-pressure ionization chambers. Thermoluminescent dosimeters are also used at several laboratories for this purpose.

For the SSC, there was general agreement that mobile muon telescopes would be needed to identify muon beam profiles. In some fixed monitoring stations (e.g., downstream of beam dumps), muon telescopes might be valuable. In other stations, gross low LET (photon plus muon) measurement would probably suffice.

Low intensity muon measurements at the SSC may pose some technical problems because it may not be possible to use accelerator-cycle gating pulses to improve the signal-to-noise ratio, as can be done for example at FNAL.

Van Ginneken reported on the extension of his muon calculations for primary proton energies of 40 TeV (Appendix A.4). No great surprises were found.

2.3 Gas, Dust and Aerosol Activation

O'Brien reviewed his work on the computation of the atmospheric inventory of ^{7}Be, ^{10}Be, ^{14}C and ^{85}Kr produced by cosmic radiation. In general, excellent agreement with observation is obtained. (Appendix A.7)

Moritz (TRIUMF) described experience at TRIUMF. As a rule of thumb, neutron fluence rates in the range 10^5 - 10^6 $ncm^{-2}s^{-1}$ will theoretically produce concentrations of radionuclides (^{3}H, ^{7}Be, ^{11}C, ^{15}O, ^{13}N and ^{41}Ar) close to the ICRP 'Derived Air Concentrations'. The radionuclides are generally of low radiotoxicity and, except for 12.3 year ^{3}H, of short half-life. Even low ventilation rates generally militate against saturation being achieved for the longer-lived radionuclides. As a general rule, ^{7}Be is found at much lower concentrations than predicted. The reason for this is not entirely known but probably is due to plating down of particles to which ^{7}Be attaches itself. ^{7}Be is routinely found at low concentrations in dust and in filters at accelerator laboratories.

Moritz drew attention to the conflicting goals of reducing exposure to workers in experimental areas (high ventilation rates) with that of reducing exposure to other workers on-site and the general population (low ventilation rates). This apparent conflict must be considered in the design of ventilation systems and administrative controls. TRIUMF annually releases ~1 kCi of the short-lived radionuclides as does FNAL.

Although it is generally true that exposure to workers in accelerator environments is dominated by the induced radioactivity of solid materials and not by immersion in a cloud of radioactive gas, Stevenson (CERN) pointed out that it is possible to generate considerable gaseous radioactivity by passing

pencil beams through air without inducing much radioactivity in the surrounding structures. Casey (BNL) reported problems with ^{38}Cl and ^{39}Cl production where proton beams are passed through air.

Fasso (CERN) reported experience at CERN (Appendix A.5). Changes in the approach to monitoring have evolved as the problem of gaseous radioactivity has increased. At the SC, thermoluminescent dosimeters are used to monitor the effluent stack. Aerosol and gaseous radioactivity are monitored using charcoal filters at the SPS which is ventilated continuously. Both FNAL and TRIUMF have continuous stack monitors using thin window geiger counters on NaI detectors in shielded chambers.

It was pointed out that if tunnels and below-ground enclosures are not ventilated continuously, radon accumulation may become a problem. Pagenais (FNAL) has calculated that without ventilation radon would accumulate to greater than 600 pCi/l leading to exposure rates greater than 10 mR/h.

Stapleton (CEBAF) pointed out that corrosive products may be produced in areas of high-radiation fields, especially at high relative humidity. To minimize this at CEBAF, dehumidified air will be circulated and ventilated usually only after a delay. This will also provide several hours of delay with a consequent reduction in the release of radioactivity to the environment.

2.4 Ground Water Activation

Baker (FNAL) discussed measurements of activity in earth and water, made adjacent to an Abort Dump region in 1973 and 1983 (Appendix A.9). About 3 x 10^{18} protons had been directed to the abort dump. Principal efforts have been made to study ^{3}H and ^{22}Na that are the radionuclides most easily removed by leaching from activated soil. Measurements found concentrations of ^{22}Na and ^{3}H at beam height in adjacent soil and water. Peak concentrations were 200 pCi/g (^{22}Na) and 50 pCi/ml (^{3}H). CASIM calculations predicted these observations within 20%. At three feet farther from the tunnel, the prediction for ^{22}Na was 20 pCi/g and the measured value was 9 pCi/g. No significant activity was measured in the water in the drains below the abort-dump -- indicating little leaching downward. This low leach rate is believed to be due to the protective overburden of clay.

Column experiments in sand and gravel indicate that 6% of the ^{22}Na is leachable (to be compared with estimates of 20% in finely divided soil). The total amount of ^{3}H in the soil has not been determined, as only the leachable amount is measured. Other radionuclides, e.g., ^{7}Be, ^{45}Ca, ^{54}Mn, ^{60}Co, are observed but do not appear to be significant. ^{22}Na has now been observed in vegetation growing on beam dumps at concentrations of 0.1 - 10 pCi/gm (dry weight).

The Fermilab experience is that the measured ratio of ^{22}Na to ^{3}H in water from underdrains below the primary target ($\leq$ 0.001) is smaller by a factor of five or more than would be expected from the pick-up in unirradiated soil measured by Borak et al. (Appendix A.12) BNL has observed a higher ratio ($\simeq$ 0.005) of ^{22}Na to ^{3}H in a well about 1 km from the AGS.

For the DESY accelerator HERA, the accelerator ring which follows the level of the terrain is situated in the aquifer in most places. Hamburg does not have small volume wells used by individual families as a source of drinking water: All drinking water is provided by the City Water Board. Any ^{3}H or ^{22}Na which might be leached into the community drinking water supplies will thus be diluted in very large volumes of drinking water.

Baker stressed the importance of understanding that each site is different, and that the quantitative implications of radionuclides in water can only be understood when the details of geology and hydrology are known. For example, at a site where large volumes are pumped from local aquifers there is great dilution resulting in lower concentrations than at sites where small volumes of drinking water are derived from aquifers close to the accelerator.

Baker presented the results of a rough estimate of the activity produced in a low yield well (40 gals/day) adjacent to a reservoir in which an accidental full loss of beam occurs (3.9×10^{14} protons). He estimates concentrations of 14 pCi/ml for ^{3}H, close to drinking water standards. The worst case ^{22}Na level is 3.5 pCi/ml; that is higher than the EPA concentration corresponding to 4 mrem/yr in a drinking water supply.

Cossairt (FNAL) presented the results of calculations using the Moyer Model, and compared the result with CASIM calculations (Appendix A.15). He finds agreement within a factor of three. Such agreement suggests we have adequate data to make reliable predictions

The calculation of groundwater activation and the resulting consequence to water supplies is fraught with many uncertainties. There is often a

temptation to construct highly conservative calculational models and to compound this conservatism by inserting equally conservative estimates of the several parameters of the model. This procedure may lead to serious error and should only be adopted where the result is so low as to be of dismissive consequence even given all the conservative elements in the estimate. This is frequently not the case in groundwater activation where the application of state EPA regulations may require very low limits to the activity of water beneath the facility's property. It is recommended that the calculation be done as well as possible, while maintaining an appreciation of the uncertainties in the method. Any desired margins can be applied to the end result taking these uncertainties into account at that stage.

2.5 Philosophy of Environmental Monitoring

Stevenson (CERN) discussed experience at the SPS and its relevance and implications for the SSC (Appendix A.3). CERN practice is to use both active and passive radiation monitors as part of their environmental surveillance program. In particular, active monitors are positioned close to venting points of radioactive gas release (roughly "upwind" and "downwind").

The active detectors are standard (high pressure Argon chambers; Andersson-Braun) and situated at critical points. CERN buys land or obtains easements to place passive detectors, and employees take passive detectors home to quantify natural background. Thomas commented that moderated ^{6}Li-^{7}Li TLD pairs had relatively low sensitivity for neutrons, but Stevenson explained that they were used to demonstrate compliance with CERN environmental limits (150 millirem per annum).

There was considerable difference of opinion as to whether there was a need to do "off-site" monitoring. Stapleton (CEBAF) was content to have the Department of Health (Commonwealth of Virginia) carry out off-site compliance assurance. Jenkins (SLAC) saw no need for off-site monitoring when site perimeter dose equivalent rates were as low as 10 millirem per year. Cossairt worried about "false positives" that might be produced by other agencies and felt limited off-site monitoring might be necessary.

2.6 Conclusion and Recommendations

The sources of ionizing radiation of concern to the environment for the SSC appear to be well identified. Extrapolation from experience at existing accelerators will provide an adequate means of qualifying these radiological impacts.

Skyshine phenomena are adequately understood so that dose equivalent rates from radiation streaming from penetrations in the shielding can be estimated with sufficient accuracy. It will be important to ensure that source-to-site boundary distances are consistent with environmental radiation limit design goals.

Areas where muons may occur can be predicted by calculation and their presence confirmed by measurement. Agreement between practice and theory is adequate. Site specific design factors will have an important influence on the design of beams to ensure that unwanted radiation levels due to muons emerging into the air cannot occur. It is recommended that muon range straggling and dispersion measurements be made at FNAL (1 TeV) to verify theoretical calculations.

Sufficient data are available for quantitative estimates of gaseous radioactivity. The source term can be adequately determined: administrative and operational procedures governing release and ventilation will to some extent be determined by specific site considerations. Containment and release procedure should take into account the natural radon inventory in the air and water from underground enclosures. Beam design and target layout should minimize the passage of hadrons through air.

The concentrations of radionuclides in ground water, and their transport to potential drinking water supplies will be determined principally by both the geological and hydrological characteristics of the site. Environmental data from existing accelerators are well understood and provide a reasonable basis for estimations for the SSC. Provision for the acquisition of water samples (necessary easements, installation of monitoring stations, drilling wells, water sample collectors) should be included in the final design. Baseline measurements should be made before operation. Coordination with state officials on environmental monitoring programs is most important.

Chapter 3

SUPERCONDUCTING COMPONENTS

Introduction

The use of superconducting magnets in accelerators requires that beam losses be minimized to prevent quenches induced by radiation heating. Detailed analysis of energy deposition in the magnets have been required to understand this subject fully. This session was devoted to a review of these studies. Presentations were made by A Fasso (CERN), A. Van Ginneken (Fermilab) and D. Groom (CDG). Comments on the BNL design for ISABELLE were made by A. Stevens (BNL).

3.1 Energy Deposition Calculations for the LHC Dipole

Energy deposition in the LHC dipole has been studied at CERN. The dipole was simulated in combinational geometry (Figs. H, I -- see Appendix B.1). The calculation was made using the code: FLUKA + EGS. A pencil beam was assumed incident at a grazing angle of 7 mrad onto the synchrotron radiation shield. No magnetic field was assumed. Two sets of calculations were made: one at the circulating beam energy (8 TeV) and one at the injection energy (500 GeV). Energy deposition calculations scored grossly in longitudinal "slices" of one meter thickness were made.

More detailed binning was done in the horizontal mid-plane. The results have shown a strong dependence on the selected bin size. The results shown in Appendix B.1 (Figs. J and K) refer to a volume with dimensions comparable to those of a single superconducting strand (2 mm vertical, 1.7 mm horizontal, 100 mm longitudinal). Figures L and M refer to the average over the whole inner coil radial thickness (i.e., ten times larger). The radial dependence

is shown in Figs. N and O, and summarized in Tables P and Q. The latter tables also report for comparison early values calculated with smaller bin sizes at 10 TeV.

To estimate allowable losses, the maximum calculated energy densities were assumed to occur over a distance equal to the longitudinal full width at half maximum (FWHM) for a single incident proton. Figure R shows the estimated maximum loss at 8 TeV and 500 GeV under the two different assumptions that the single strand or the whole inner coil is the element of concern for magnet quenching. To calculate these values, the assumed enthalpy reserve at the two energies was taken from available ISABELLE calculations.

More accurate calculations should take into account realistic angular incidence of the protons, magnetic field and time bunch structure of the beam. The total heat load of the dipole from losses too low to quench the magnet is also possibly of some importance.

3.2 Monte Carlo Calculations of Radiation-Induced Heating in Magnets

Radiation induced quenching due to beam losses at extraction was studied at Fermilab (A.V. Ginneken, D. Edwards, H. Edwards, M. Harrison -- to be published) both during design and operating stages of the superconducting ring. This study proves that for a known mode of beam loss, the problem is well-understood by means of Monte Carlo simulations of the beam loss and the subsequent energy deposition in the coils of superconducting magnets. While a truly quantitative fit to observation is not achieved, this may be traced back to the sensitivity to precise placement of the magnet with respect to beam position.

The known beam loss mode is a small (~1-2%) fraction of the beam that strikes the wires of the electrostatic septum at extraction. This creates two distinct problems: (a) particles emerging from inelastic collisions which strike the accelerator components immediately downstream of the septum and (b) protons which scatter elastically and which either follow the beam for up to 2-1/2 turns before being extracted, or else accumulate at certain "hotspots" around the ring where large horizontal excursions take place. Both problems are addressed by the simulations. Comparisons with experiments are performed for the elastic component at a few (typical) hotspots. Quench levels agree with each other and with nominal design values (which are, in turn, based on calculation and experiment) to within a factor of two. Simulation of energy deposition in beam loss monitors proved to be essential to arrive at these comparisons. Both types of losses (i.e., losses near the septum and ring-wide losses) are, to a great extent, cured by collimation.

At the SSC, there exist sources of beam loss which are likewise easy to simulate, i.e., elastic and inelastic interactions in the IR's, and with beam gas around the ring. Slow orbit growth (due to various other effects) and subsequent capture on clean-up collimators forms another source of radiation which is harder to calculate. Nonetheless, considerable progress is being made at present (A. Van Ginneken, M. Harrison) on similar problems at the Tevatron, and additional tools developed expressly for this study could be helpful in making predictions for the SSC.

3.3 Measurement of Neutron Spectra in the Tevatron Tunnel

Groom reported on a new measurement of neutron spectra and dose in the Tevatron tunnel. This was the latest in a series of measurements (Appendix B.3) designed to determine if semi-conductor control circuitry and detectors (e.g., quench protection diodes, temperature sensors, beam position monitors) located within the accelerator-magnet enclosure will be damaged by the internal radiation environment. This environment has a mixture of sources (e.g., beam-gas interactions, beam-beam interactions in the Interaction Regions, and beam interaction with localized targets such as collimators or scrapers). In most areas of the SSC tunnel, the radiation environment will be dominated by the beam-gas interactions, and the purpose of these measurements was to evaluate this contribution.

Several improvements to the experiment were made in the measurements. In particular, neutron rates from beam-gas interactions and other sources were separated by measuring counting rates as a function of gas pressure. The pressure in a warm section was set by a remotely controlled ultra-high vacuum leak.

These measurements yielded results close to those predicted in ORNL simulations (HETC, MORSE) for the energy of secondary neutrons and for the production rate. The neutron spectrum is sharply peaked at an energy of about 700 keV. The measured rate suggests that beam-gas interactions would produce a fast neutron ($E > 0.1$ MeV) fluence of 1420 n $cm^{-2}s^{-1}$ in the tunnel with 10^{14} protons circulating in a vacuum of 10^{-8} Torr. This value can be compared with the estimate of 2000 n $cm^{-2}s^{-1}$ based on extrapolations of previous PPA results and the value of 8000 n $cm^{-2}s^{-1}$ estimated from the 1985 measurements in the Tevatron tunnel.

These preliminary results suggest that in a typical operating year, semi-conductors will experience a flux density of $\sim 3 \times 10^{10}$ n/cm^2. The implication to SSC is that components will need to be carefully selected (e.g., some components can fail in the range of $10^{11} - 10^{12}$ n/cm^2). Local shielding of components may be desirable and achieving vacuum at 10^{-8} Torr is quite important.

3.4 Implications for SSC

Codes such as CASIM and FLUKA provide increasing capabilities of predicting radiation induced heating. The ORNL codes (HETC, MORSE) give increasing confidence in the ability to accurately determine neutron spectra for known sources of loss. Taken together, this means that excellent tools now exist for detailed studies related to the quenching of SSC magnets and to the possible damage to SSC components. Although these studies, specified below, will take a great deal of effort, the important point is that tools are available. Nothing was discovered, or suggested, that would indicate interference with normal SSC operations.

3.5 Issues/Future Studies

1. Sources of Loss

Although "catastrophic" loss was discussed in this Workshop in conjunction with personnel and public protection, additional attention should eventually be given to the effect on the superconducting magnets of known or probable losses. As an example, septa and collimators intrude into the vacuum chamber. It is possible, using the enhanced abilities of CASIM, to calculate how much loss on such objects could be tolerated without quenching magnets. Although such calculations are subject to a variety of uncertainties, we believe that the exercise of going through "loss scenarios" is one well worth making, so that some estimate of tolerable or acceptable beam loss can be obtained.

2. Location of Solid State Components

Given reasonable loss scenarios, and our confidence in the ability to calculate neutron spectra, an expected (or tolerable) "radiation map" could be prepared, i.e., values of dose or fluence as a function of position in the tunnel. Questions related to the survivability of cold diodes and other electronic components could then be answered. An excellent start has been made in the preliminary beam-gas studies reported by Groom et al. The contributions from other sources should also be assessed. These studies may have an impact on alcove design and on the necessity to employ beam loss monitors or other dosimetry systems in certain portions of the ring.

3. Tritium Production/Induced Radioactivity

The issue of tritium production was on the agenda, but was not fully discussed. Given reasonable loss scenarios, the ability to calculate spectra

with such programs as CASIM and FLUKA, and tritium production cross sections, some estimates could and should be made. Based on preliminary calculations made at CERN (Appendix B.4) and on operating experience at FNAL, this is not believed to be a problem. However, further studies should be done for completeness.

In addition induced activity in some ring components might be calculated. However, previous calculations (see note by A. Stevens in Appendix B.6) and FNAL experience would indicate that no problems are anticipated.

3.6 Conclusions

The concept that the sensitivity of superconducting magnets limits beam loss to extremely low values was certainty not questioned in this Workshop. The FNAL Tevatron experience has been enormously encouraging - proving that beam loss can be held low enough for the accelerator to work well. The SSC CDG is to be commended for paying great attention to this topic well in advance of construction; they are much further "ahead of the game" than, e.g., the Tevatron was at a similar stage in development.

Rapid advances have recently been made in the ability to calculate energy deposition densities given known sources of beam loss. These provide tools for detailed studies on the SSC.

It is important to recognize that these studies will represent a new phase of detailed design which goes beyond the motivation (site selection) for this Workshop. A good starting point for this next phase would appear to be models for losses associated with slow beam growth.

Chapter 4

BEAM ABSORBERS (DUMPS)

4.1 Summary of Presentations

In this session, the following topics related to the design of the beam abort dumps were discussed: (1) energy deposition (heat and radioactivation), (2) mechanical damage/dump integrity, (3) use of upstream dispersive absorbers, (4) activation of cooling water, (5) ground water activation, (6) dump monitoring, and (7) containment of the prompt radiation.

The abort design as illustrated in the Conceptual Design Report (SSC-SR-2020) was reviewed by J.D. Cossairt (see note in Appendix C.1). This review concluded that the assumed physical size of the shower is approximately in accord with calculations appearing in Fermilab FN447 by Van Ginneken et al. Simplistic calculations of the expected temperature rise also appear to be correct, and manageable. The activation of cooling water was examined. For this postulated core of graphite, the radioactivation was calculated. A calculation of ground water activation at equilibrium near a possible concrete shield surrounding the dump was made, with a resultant size suggestion for this shield. Finally, the report by Van Ginneken et al. was used to show the shielding requirements needed to handle the prompt radiation for both hadrons and muons.

Van Ginneken summarized recent work he has done (transparencies in Appendix C.2) which is being published (A. Van Ginneken, Nucl. Instr. & Meth. A251 (1986) 21, and S. Quian and A. Van Ginneken, Fermilab Pub 86/145, October 1986, to be published in Nucl. Instr. & Meth.). The work studied energy loss mechanisms such as muon-nuclear inelastic scattering, bremsstrahlung, direct

pair production and nuclear interactions of muons. Since some of these mechanisms become more important for E > 1TeV, procedures for incorporating them into reasonably efficient Monte-Carlo procedures were presented. The implications for angular distributions are now reasonably well understood, and have been compared with other work.

Graham Stevenson summarized work done for the LHC aborts (see Appendix C.5 for transparencies). Here the design constraints are quite tightly defined because the location in the LEP ring is specified. Many studies of absorber materials have been done which are of direct benefit to the SSC. Graphite has been selected, somewhat reluctantly, over aluminum, water, and lithium. Energy deposition calculations with FLUKA have been made that are broadly consistent with CASIM. CERN, too, has concluded that significant geometrical dispersion of the 8 TeV beam on the dump face is necessary.

Sam Baker submitted a 1975 report (see Appendix C.6) of soil activation measurements at Fermilab that describes a monitoring program for a large proton beam dump in the Fermilab Neutrino area. A further discussion is contained in a summary (see Appendix C.7) of operations at Fermilab from 1972 to 1982. This note concludes with observations about shielding design and monitoring requirements for large beam dumps such as the SSC aborts would be.

4.2 Implications

1. The sizing of such beam dumps from considerations of shower energy absorption, ground water activation, and prompt radiation seems to be well understood. Especially if graphite is used, its density must be well known.

For ground water protection, it is clearly perferable to size the shield to achieve the desired estimated concentration without resorting to impermeable membrane barriers.

2. Water cooling loops may be designed so that they are similar to those in present installations. This water would be activated to the same levels that are presently successfully handled at high-energy accelerators. Any plumbing should be kept inaccessible to personnel to prevent exposure due to short-lived radionuclides.

3. Activation of the dump core will be within reasonable limits so long as low Z materials (BeO, Li, H_2O, C, ...) are used. Natural lithium may have a problem due to thermal neutron capture by ^6Li which copiously produces ^3H.

4. Provisions for monitoring activation levels and movement of water in the dump environs should be built in. Under drains would be of great value for this purpose.

5. Instrumentation is necessary to verify proper performance of the kickers and defocussing quadrupoles. It would be prudent to have retrievable beam monitoring instrumentation downstream of the dump to verify its integrity. To avoid large-scale contamination of the collider, the large window should be monitored to initiate appropriate corrective actions should it fail.

6. The participants briefly discussed the use of dispersive absorbers in the abort beam line. This alternative to some of the kickers seems unattractive in that absorber providing significant beam smearing would simply translate the dump problems to less desirable locations upstream of it.

4.3 Suggestions for Future Studies

1. If graphite is chosen for the absorber the problems of successful thermal contact, of the need to "anneal" it to remove stored energy, and of depletion of its density by repeated heating merit considerable, detailed studies. These problems may be dependent upon the macroscopic form of the graphite. Alternative absorbing media will have different problems to be considered.

2. Beam monitoring instrumentation must be designed for reliability so that proper operation of this dump can be assured.

3. A complete failure - mode analysis will be needed at the appropriate time to provide assurance that the dump can operate properly. This would, among other things mentioned here, examine in detail the effects of failures of abort components upon these radiological concerns.

4. More detailed considerations of a monitoring program for ground water activation and prompt radiation will be needed. The requirements will become clearer when a site is selected. It is clear that some accessibility to the region downstream of the abort, even to the end of the muon zone, might be needed, depending upon details of the specific site choice.

4.4 Conclusions

It is concluded that the problems of the abort dump are well understood, are manageable, and are within the range of present experience and technology. There is obviously significant work to be done in a straightforward manner. We are confident that a successful design will be developed.

Chapter 5

INTERACTION REGIONS

In this session of the workshop, the following subjects were addressed: (1) dose absorbed by and resulting damage to the detectors in the Interaction Regions (G. Stevenson Appendix D.2), (2) the design of penetrations through the shielding (D. Cossairt, Appendix D.5; G. Stevenson Appendix D.1), (3) the design of the lateral hadron shield (K. O'Brien Appendix D.19; G. Stevenson, Appendix D.10), (4) the problems associated with depleted uranium (W. Freeman, Appendix D.12; T. Borak, Appendix D.17), and (5) the description of the essential features of an Interaction Region (D. Groom, Appendix D.1).

5.1 Radiation Dose to Detectors

The detectors used in the Interaction Regions are closest to the highest energy collision region in the machine and are exposed to a substantial flux of secondary particles. This poses two problems. The first is the adequacy with which the secondary particle-energy distribution can be described from a source of essentially unprecedented energy and substantial intensity. The second is the calculation of the damage to be expected in the electronics.

A study of the latter problem awaits the solution to the former. Calculations were carried out using the model known as PYTHIA, devised at Lund by Bengstrown et al., and ABR8506, devised by Ranft based on work by Aurenche relevant to 10 and 20 TeV (LHC and SSC energies, respectively) (see Appendices D.2 & D.3). These models were used to generate files of source particles that were transported, using FLUKA, through a model of the detector surrounding the IR. The model was necessarily simplified and represented as a spherical shell of aluminum.

At 10 TeV, the power dissipation was taken to be 320 W and at 20 TeV twice that. The resulting annual dose rates at certain positions will be quite high (see Appendix D.1 and D.2): sufficiently large to render most solid-state electronic circuits useless, to darken optical fibers and plastic scintillators and to cause damage to silicon radiation-detectors. (See Appendix D.4 for references.)

A review of radiation damage studies indicates the need to investigate the effects of radiation on appropriate scintillating and other materials of interest in an environment as close as possible to the expected conditions. (See Appendix D.4.)

5.2 Labyrinths, Ducts, and Penetrations

In any well-shielded accelerator environment, the proper design of shielding penetrations such as labyrinths (for personnel access and cable ducts) is critical. It is perfectly possible to simulate the geometry and source-energy distribution in a computer-readable format and calculate radiation propagation from first principles. This is both difficult and extremely time-consuming. Such calculations, however, along with experimental data and some elementary physical principles, have led to two layers of simplification. The first is the discovery that after the first bend in a penetration, neutrons with energies of a few MeV dominate the dose equivalent, leading to an enormous simplification in the source description. Codes exist having an albedo option (replacing particle-nucleus collision modules with doubly-differential albedo cross sections at material surfaces) and an appropriate neutron energy-source distribution for calculations of dose attenuation through penetrations. In the second layer of simplification are the formulae developed at a number of laboratories that treat the dose along the legs of penetrations empirically and, in some cases, with high accuracy.

All three layers of complexity are important because of the need of varying requirements of speed in obtaining results, the need to assure consistency, and the need to explore non-standard configurations.

In this Workshop, Cossairt used attenuation curves developed at Fermilab using the ZEUS mono-energetic albedo transport code to predict attenuation in passage-ways leading to the Interaction Region experimental areas of the SSC (Appendix D.5). He also demonstrated the applicability of the method in a labyrinth experiment at Fermilab (Appendix D.6). Stevenson presented a summary

of experimental and theoretical duct attenuation work at a number of high-energy accelerators (Appendix D.7) showing that the ZEUS albedo hadron generally over-estimated the degree of attenuation in a multi-legged labyrinth and proposed generalized attenuation curves based on a wider range of experience. He also showed how these curves compared with attenuation measured in a complicated duct at the CERN SPS (Appendix D.8).

5.3 Lateral Hadron Shielding

The side shielding of accelerators with energies below those of the SSC (relevant to the problem of radiation from the SSC's injectors) is calculated using a picture of the transverse-energy distribution based on CKP-like formulae. These formulae predict a relatively low energy essentially neutron component exiting from the sides of targets and of accelerating structures (Appendix D.19).

Straight-ahead, discrete ordinates, spherical harmonics and Monte Carlo solutions of the Boltzmann equation have been carried out and are in substantial agreement for neutron propagation at ranges exceeding 1000 g/cm^2 (Appendices D.9, D.19).

CKP-type formulae, such as the one developed by Ranft and Borak based on some earlier work by Trilling, lead to a transverse-energy spectrum that is largely independent of accelerator energy and, hence, rather easily generalized. Since the physics describing particle-nucleus collisions changes drastically as one descends in energy below a broad region centered at a few hundred MeV, it is useful to write codes that focus on energy regions above and below this area. When this is done high-energy codes used where the neutron-only assumption is invalid can be coupled with those lower energy codes to obtain an adequately precise picture of the neutron-energy spectrum from the highest energies down to thermal energies (Appendix D.11). In addition, of course, some of these higher-energy codes can be easily used for the same sort of side-shielding calculations described above (Appendix D.19).

As in the case of penetration calculations, a further simplification is possible. In the late '40's and early '50's, B. Moyer noted that ~150 MeV neutrons had a substantially greater interaction length than those with much more or much less energy; as such, they "carry" the radiation from one point in the shielding to another, where subsequent shorter-range interaction produce the observed radiation. This picture is the basis for the exponential-kernel line-of-sight approximation known as the Moyer Model. Its parameters have been adjusted by careful comparison between the results obtained with a rigorous high-energy Monte Carlo code, (FLUKA) and experimental studies. The method is easily applied, and with the usual addenda of experience and common sense can be readily used with some confidence to solve complex problems (Appendix D.11).

The conversion of hadron flux data to dose or dose equivalent is based on calculations of dose or dose equivalent resulting in a phantom when exposed to radiation of various types and energies. Such calculations have been carried out for phantoms of various descriptions, for fluxes of varying angular composition, and have been related to differing regions of the phantom. Hence, not all flux-to-dose equivalent rate calculations are quite the same (Appendix D.10).

5.4 Problems with Depleted Uranium

A review of the uranium handling experience from assembly of the prototype liquid-argon-depleted uranium calorimeter for E-740 at Fermilab was presented.

Various work activities were identified, including measurement of uranium plate dimensions, squareness and flatness, attachment of electrical leads, bonding of G10 to uranium plates, welding tests, and cryogenic cycling of materials. A general summary of this study is given in (Appendix D.15).

Typical dose rates from plates as well as a summary of personnel radiation exposures are given in the attached copies of transparencies (Appendix D.12). More details are provided in Appendices D.13 and D.15. The importance of maintaining plates in an environment with reasonably low humidity and at room temperature to prevent excessive surface oxidation was emphasized (Appendix Ref. D.14) The whole problem of excessive removable activity (the surface oxidation) can be greatly reduced if coated plates are used. (See Appendix D.13, pg. 3.)

Some "highlights" of uranium handling experience at other laboratories are reproduced in the attached transparencies (D.12). Potential contamination and fires resulting from the pyrophoric nature of small uranium chips and flakes are the main concerns, as is the flammability of bulk uranium if temperatures high enough to ignite it can be reached. As a result of these considerations, no machining, (filing, cutting, drilling, sawing. etc.) of uranium is allowed on the Fermilab site. Only assembly of modules by stacking finished plates is currently permitted. This policy will be extended to the full calorimeter assembly operation as well.

Welding tests on uranium were attempted with generally poor results. Extensive air sampling during the welding operations showed airborne concentrations that would approach annual limits if done on a routine, continuous basis. Especially troublesome from an airborne concentration point of view were attempts to weld one uranium plate to another. Special precautions such as the use of respirators, sampling, welding in an inert atmosphere, etc., will be required for any welding operation involving uranium. It would be advisable to avoid all such operations on-site.

Cryogenic cycling of uranium plates presented little problem from a radiological perspective. Only minimal amounts of contamination were found inside the test cryostat after warming up. No radon gas buildup was detected inside the cryostat.

The planned area for assembly of the full calorimeter for the E740 (DO) experiment was reviewed and the handling process was briefly described.

5.5 Accidental Uranium Release

A paper by Borak was presented in which an initial study had been made of the effect of an accidental release of uranium in aerosol form into the environment close to CERN (Appendix D.17). After giving details of the pathways through which the uranium could provide a hazard to man and a summary of air-dispersion calculations, he deduced that a total release of 20 kg of respirable particles under stable meteorological conditions could give rise to a dose equivalent exceeding 20 mrem via the inhalation of insoluble aerosols of uranium. During worst-case meteorological conditions, this same dose equivalent would be exceeded by a release of 7 kg of respirable aerosols. The limits for chemical toxicity are similar.

5.6 Accelerator Shielding Prospectives

Accelerator side-shielding is governed by the transverse-energy distribution resulting from the collision of the accelerated particles in the target or accelerator structure. The CKP-like formulae that describes these distributions at sub-SSC energies are functions of secondary energies alone and very soft. This has important effects: The transverse-energy distributions of all such machines (with accelerating energies > 800 MeV) are alike. As particles are lost and cascade through the interior of the machine, the transverse-energy distribution remains unchanged, and only neutrons need be considered.

To exploit these phenomena, one must know the number of stars (i.e., inelastic collisions) produced on average by a particle in matter. Calculations indicate that for collision energies above 100 MeV, the number of stars is proportional to energy

$$V_* = 2E,$$

where E is in GeV.

The source-energy distribution was taken from a formula based on work by Trilling, Ranft, and Borak. This served as the boundary condition on the inside of the shield. The outside of the shield was assumed to be in vacuum.

The Boltzmann equation and the appropriate absorption, scattering, and inclusive production cross sections were expanded in spherical harmonics. Considering them and utilizing the addition theorem leads to a second order ordinary differential equation that was solved analytically for each energy group and then summed over energy.

The results of this treatment were in satisfactory agreement with calculations of others and with experimental data.

A table was prepared based on the above considerations that would allow the determination of the dose equivalent rate outside an arbitrary accelerator shield once machine energy, beam loss, and shield water content were known.

5.7 Issues, Future Study and Conclusions

The high-energy, high-luminosity p-p colliders now being designed present new radiological issues because of both of these factors. At the SSC, a given lost proton produces about 13 times as much radiation as a lost proton at the Tevatron, and the number of protons per second passing a given point will be about two orders of magnitude higher. For the first time, IR collisions dominate beam lifetime. All of this means that "beam losses" in the IR are exceeded only by those in the abort dump and possibly the injection lines. The IR-related issues addressed in this Workshop underscore the importance of the problem, and the work described above represents a serious attempt at quantitatively addressing the problems.

The 4π detector(s) will be large, and it is traditional for physicists to choose materials on the basis of properties unrelated to toxicity, chemical reactivity, or other safety considerations. Thus, in addition to beam-associated hazards to people and apparatus, there are a variety of safety problems including the radiological and chemical problems associated with large uranium calorimeters. These safety concerns should be injected into future detector planning sessions, and perhaps into laboratory policy.

In the following, we summarize a variety of radiological aspects of the future interaction regions, emphasizing also the issues which have not been addressed at this Workshop and which need to be addressed at the appropriate time.

1. Beam losses.

   The product of design luminosity, inelastic p-p cross section, and machine energy is about 800 W at the SSC, and about half this for the LHC. Since the number of particles going into each rapidity interval

is about the same, the distribution peaks sharply forward and backward along the beam direction. There are a number of implications.

(a) Energy deposition in interaction-region magnets. Most of the charged particles are swept out of the beam pipe in the focusing triplets in the IRs. Since these elements are superconducting, there are heat removal and quench considerations. The materials from which these elements are constructed must be chosen for radiation resistance. More attention to the details will be required at some future time.

(b) Activation of scrapers, magnets, detector parts, etc. To date, no detailed calculations exist, although preliminary estimates have been made[12] on the basis of beam stop calculations.[13]

(c) Radiation damage to detectors, readout electronics, etc. Stevenson's work provides the only data yet available; it was presented in this Workshop and is available as Ref. 14. The detector was modeled as a spherical aluminum shell 3 m thick and with inner radius 2 m. The picture presented above is confirmed: Maximum annual doses of 100 grays are insensitive to angle at angles greater than 30°, but rise to 10^6 Gy/yr at the most forward angles studied. Materials such as scintillator will not survive at forward angles (say less than 10°). Further calculations must proceed hand-in-hand with practical detector designs, and what is placed where will depend upon the expected dose.

(d) Activation of components and air. As mentioned above, the necessary studies have yet to be made. It is expected that forward pieces of the machine and detectors will present a radiation hazard when they are "unclothed" in the process of accessing the detectors.

2. Personnel protection

(a) Access labyrinths, interlocks, etc. The labyrinth problem presents no new features, and is a straightforward extension of work already published.[15] Presentations by Cossairt and Stevenson addressed these problems, as summarized above.

(b) Temporary shields. During work on the detector, uncovered components (e.g., the front triplet element and the front scraper) may present unacceptable radiation hazards. In this case, one could imagine temporarily covering them with local shielding. Work on this subject is needed in conjunction with the activation studies.

(c) Side shielding. A large 4π detector will provide much of its own side shielding. This is not true for IRs in which a detector has not yet been installed, or an IR containing other than 4π detectors. There are two parts to the problem: Accidental full loss of the beam, and "normal" radiation from the collision point. In the case of some IRs under discussion, personnel protection in the event of an accidental full beam loss would require at least 5 m of concrete as a temporary shield over a rather large area that would be cumbersome and expensive as the least of its inconveniences. In practice, the loss would probably occur as the beam either enters or exits the focussing

triplet. A solution could be an oversize beam pipe to escort beam-loss debris safely through the region. The triplets could be shielded, and the overall problem would be much simpler. The beam-beam collision is more problematical. It must be considered, but it is extremely difficult to unintentionally collide the beams -- obtaining luminosity in an unused IR would require a conscious effort equivalent to an interlock bypass.

3. Detector-associated problems

The only problem presently being assessed is that of massive depleted uranium calorimeters. The problem is of more relevance during fabrication than during operation, since a multiple contingency would be necessary to ignite uranium already in place in the detector. However, both problems need serious study.

REFERENCES

[1]Report of the 20 TeV Hadron Collider Technical Workshop, Cornell University, March 28-April 2, 1983.

[2]Report of the Reference Designs Study Group on the Superconducting Super Collider, DOE/ER-0213, May 1984

[3]SSC Conceptual Design, SSC-SR-2020, March 1986

[4]Invitation for Site Proposals for the Superconducting Super Collider (SSC), DOE/ER-0315, April 1987

[5]SSC Workshop on Environmental Radiation, 14-18 October 1985, SSC-SR-1016, 9 January 1986

[6]SSC Environmental Radiation Shielding; Task Force Report, J.D. Jackson ed., SSC-SR-1026, July 1987

[7]Moyer, B.J. "Evaluation of Shielding Required for the Improved Bevatron," UCRL-9769 (1961).

[8]Rindi, A. and R.H. Thomas (1975) "Skyshine -- A Paper Tiger," Particle Accelerators 1, 23.

[9]Patterson, H.W. and R.H. Thomas, (1973), Accelerator Health Physics, Academic Press, New York.

[10]Lindenbaum, S.J. (1957) "Brookhaven National Laboratory Proton Synchrotron, USAEC Report TID-7545, p.28.

[11]Jenkins, T.M. (1974) Accelerator Boundary Doses and SKYSHINE , Health Physics 27, 251

[12]Groom, D. E. (1986), SSC Central Design Group Note SSC-N-219.

[13]Gabriel, T. A. and R. T. Santoro (1973), Particle Accelerators 4, 169-186.

[14]Stevenson, G. R. (1987), CERN Report TIS-RP/188/CF (LHC Note 46) [Appendix D.3].

[15]Stevenson, G. R. (1987), CERN Report to be published in Proc. of ANS Conf. Knoxville, TN (April 22-24, 1987) [Appendix D.7].

APPENDIX A Environment and Monitoring

A.1 L. Coulson, W. Freeman, and T. Toohig, A guide to understanding the radiation environment of the Superconducting Super Collider (SSC), DRAFT, 1 May 1987.

A.2 A.J. Elwyn, Muon fluence measurements at the site boundary for 1985, Fermilab TM1394.

A.3 Viewgraphs, G.R. Stevenson, Environmental and experimental-area monitoring at CERN for stray radiation, 4/5/87.

A.4 Letter to T. Toohig from A. Van Ginneken, 26 March 1987.

A.5 A. Fasso, and G.R. Stevenson, Radioactive air releases - CERN policies and practice, 5/6/87.

A.6 A. Fasso et al., Radiation protection considerations for a large hadron collider, TIS-RP/IR/84-20, Internal Report, 28 March 1984.

A.7 K. O'Brien, Cosmogenic isotope production: implications for the radioactivation of air in the neighborhood of accelerator structures, 6 May 1987.

A.8 W.S. Freeman, Review of recent muon measurements at Fermilab, 5/4-6/87.

A.9 S.I. Baker, 8L: Fermilab soil activation experience.

A.10 Table 3, CY-1986 Sediment Sampling Results, S.I. Baker Fermi National Accelerator Laboratory Environmental Monitoring Report for Calendar Year 1986 Fermilab Report 87/58, Table 4, CY-1986 Vegetation Sampling Results.

A.11 Letter to T. Toohig from S.I. Baker, 25 February 1987.

A.12 T.B. Borak and M. Awschalom, Fermilab; F. Fairman, Iwami, and K. Sedlet, Argonne National Laboratory, The underground migration of radionuclides produced in soil near high energy proton accelerators, Health Phys. 23, 679, 1972.

A.13 A.J. Elwyn, and W.S. Freeman, Muon fluence measurements at 800 GeV, TM 1288, 11/84, Fermilab.

A.14 J.D. Cossairt and L.V. Coulson, Neutron skyshine measurements at Fermilab, Health Phys. 48, 175, 1985.

A.15 J.D. Cossairt, Unorthodox methods of calculating the activation of groundwater by routine SSC operations, April 1987.

A.16 J.D. Cossairt, Skyshine from the SSC interaction regions, April 1987.

A.17 J.D. Cossairt, and J.G. Couch, A.J. Elwyn, and W.S. Freeman, Radiation measurements in a labyrinth penetration at a high energy proton accelerator, Health Phys. 49, 907, 1985.

A.18 K. O'Brien, Secular variations in the production of cosmogenic isotopes in the earth's atmosphere, J. Geophys. Res. 84, 423, 1979.

APPENDIX B Superconducting Components

B.1 Large Hadron collider in the LEP tunnel, presented by A. Fasso.

B.2 Viewgraphs, Radiation induced quenching, presented by A. Van Ginneken.

B.3 Viewgraphs, Neutron flux measurements in the Tevatron tunnel, J.D. Cossairt et al., 22 October 1986.

B.4 G.R. Stevenson, et al., Environmental considerations for a large Hadron Collider, From TIS-RP/TM/84-16, Technical Memorandum, 9 March 1984.

B.5 A.J. Stevens, Induced radioactivity in the vicinity of an ISABELLE scraper, Brookhaven National Laboratory Technical Note No. 116, May 21, 1979.

APPENDIX C Beam Absorbers

C.1 J.D. Cossairt, Review of the abort dump shown in the SSC conceptual design report, April 1987.

C.2 Viewgraphs, Energy Deposition at Multi-TeV Energies, A. Van Ginneken.

C.3 S. Quian, and A. Van Ginneken, Characteristics of inelastic interactions of high energy hadrons with atomic electrons, Fermilab-Pub-86/145, October 1986. Submitted to Nucl. Instr. & Meth. A.

C.4 A. Van Ginneken, Energy loss and angular characteristics of high energy electromagnetic processes Nucl. Instr. & Meth. A251, 21, 1986

C.5 Viewgraphs, G.R. Stevenson, Beam dump (abort) studies for the CERN-LHC, 5/5/87.

C.6 S.I. Baker, Soil activation measurements at Fermilab, Fermilab report, 17 September 1975.

C.7 S.I. Baker, Beam Dumps, 4-6 May 1987.

C.8 N.V. Mokhov, and J.D. Cossairt, A short review of Monte Carlo hadronic cascade calculations in the multi-TeV energy region, Nucl. Instr.& Meth. A244, 349, 1986

C.9 A.J. Elwyn and J.D. Cossairt, A study of neutron leakage through an Fe shield at an accelerator, Health Phys. 51, 723, 1986.

C.10 J.D. Cossairt, S.W. Butala, and M.A. Gerardi, Absorbed dose measurements at an 800 GeV proton accelerator; comparison with Monte Carlo calculations, Nucl. Instr. & Meth. A238, 504, 1985.

APPENDIX D Interaction Regions

D.1 Viewgraphs, D. Groom, Radiological aspects of SSC operation, Interaction Regions, 5/5/87.

D.2 G.R. Stevenson, Dose to detectors in IR's, 5/5/87.

D.3 G.R. Stevenson, Dose due to p-p collisions in the LHC intersection regions, TIS-RP/188/CF, LHC Note 46, 23 January 1987.

D.4 H. Schonbacher, Review of radiation damage studies in scintillating materials used in high energy physics experiments, TIS-RP/TM/87-DRAFT 4/14/87.

D.5 J.D. Cossairt, Checking the numbers for the labyrinths shown in SSC conceptual design, April 1987.

D.6 J.D. Cossairt, et al., Radiation measurements in a labyrinth penetration at a high-energy proton accelerator, Health Phys. 49, 907, 1985.

D.7 G.R. Stevenson, Neutron attenuation in labyrinths, ducts and penetrations at high-energy proton accelerators ANS Conf., 22-24 April 1987, Knoxville, TN.

D.8 G.R. Stevenson, and A. Fasso, A comparison of a MORSE calculation of attenuation in a concrete-lined duct with experimental data from the CERN SPS, ANS Conf., 22-24 April 1987, Knoxville, TN.

D.9 G.R. Stevenson, Lateral hadron shielding at IR's, 5 May 1987.

D.10 G.R. Stevenson, Dose equivalent per star in hadron cascade calculations, TIS-RP/173, CERN divisional Report, 26 May 1986.

D.11 G.R. Stevenson, 2.5 Empirical shielding formulae, TIS-RP/GRS-LB29, To be published as ITS-RP/IR/87

D.12 Viewgraphs, Uranium handling experience at Fermilab, 5/5/87.

D.13 J.G. Couch, and R.A. Allen, External radiation dose measurements from depleted uranium, Rad. Phys. Note No. 41, 7 February 1984.

D.14 A.J. Elwyn, B. Arnold, and J. Luoma, Some observations on the dependence of surface contamination of uranium on temperature and humidity, Rad. Phys. Note No. 47, August 1984.

D.15 R. Allen, Collective external dose equivalents for uranium calorimeter fabrication, November 1986.

D.16 Fermilab Uranium Handbook, 11/85.

D.17 T.B. Borak, The environmental impact of an accidental release of uranium into the atmosphere near CERN, TIS-RP/IS/87-03, Internal Report, 23 January 1986.

D.18 D.E. Groom, A first attempt: Radioactivation of SSC final focus quadrupoles, SSC Central Design Group, SSC-N-219, 20 August 1986.

D.19 K. O'Brien, A solution to the transverse shielding problem for high-energy (>0.8 GeV) electron and proton accelerators, US AEC Health & Safety Laboratory, Preprint Presentation for 2nd International Conference on Accelerator Dosimetry and Experience, November 1969.